LITERATURE CITED

1. V. V. Kafarov, Methods of Cybernetics in Chemistry and Chemical Engineering [in Russian], Moscow (1976).
2. S. M. Aizin, A. S. Zherebovich, V. A. Falin, and V. E. Bomshtein, Teor. Osn. Khim. Tekhnol., 17, No. 3, 373-380 (1983).
3. V. A. Borodulya and L. M. Vinogradov, Combustion of Solid Coal in a Fluidized Bed [in Russian], Minsk (1980).
4. G. Borghi, A. F. Sarofim, and J. M. Beer, "A model of coal devolatilization in fluidized beds," AIChE 70th Annual Meeting, New York (1977).
5. A. Atimtey, in: Fluidization, New York (1980).
6. B. V. Kantorovich, Introduction to the Theory of Combustion and Gasification of Solid Fuel [in Russian], Moscow (1958).
7. Modeling and Analysis of Moving Bed Coal Gasifiers, AF-590, Vol. 1, Final Report (1977), EPRI.
8. D. Kunin and O. Levenshpil', Commercial Fluidization [in Russian], Moscow (1976).
9. D. Geldart, Powder Technol., 6, No. 4, 201-205 (1972).
10. S. Mori and C. Y. Wen, AIChE J., 21, No. 109, 137-141 (1975).
11. M. F. Davidson and D. Harrison, Fluidization of Solid Particles [Russian translation], Moscow (1965).
12. H.-P. Riqvarts, Verfahrenstechnik (Mainz), 7, No. 3, 164-168 (1977).
13. T. P. Chen and S. C. Saxena, AIChE Symposium Ser., 74, No. 176, 149-161 (1978).
14. D. Merrick and J. Highley, AIChE symposium Ser., 70, No. 137, 366-378 (1974).
15. "Fluidized bed combustion development facility and commercial utility, AFBC design assessment," Annual Report, EPRI Contract No. RP-718-2, Babcock Silcox Co. (1978, 1979).
16. V. N. Shemyakon, K. I. Mishina, and V. E. Kin, Problems of Heat and Mass Transfer in Furnaces, Gas Generators, and Chemical Reactors [in Russian], Minsk (1983), pp. 134-145.

INFLUENCE OF POROSITY ON THE DYNAMIC PROPERTIES OF A LOOSE GRANULAR LAYER

A. F. Ryzhkov, B. A. Putrik, and V. A. Mikula

UDC 532.546

Processes accompanying the sudden retardation of a layer with its different porosity are analyzed by using a perfected dynamic model of a loose granular medium. The results are compared with systematic experiments.

In technological processes associated with the reworking of granular media, it is usual to deal with different loose layers whose density change occurs principally because of structural deformations. In intensive methods of reworking, when the layers are subjected to some kind of mobile state, the operating density of the granular mass is less than or equal to the critical.* Under the eposidic nature of the displacements, the density of the fill increases and can approach the maximal.† Theoretical investigations of the dynamics of such systems are complex [7]. Hence in laboratories it is often obligatory, in substance, to conduct full-scale tests on equipment simulating industrial specimens. In a number of cases they can be replaeed by models. In particular, certain dynamic properties of fluidized and moving layers are simulated in an impact-disturbed stationary loose fill with an equivalent structure [3].

In order to determine the dynamic properties of a granular layer it is necessary to know its force characteristic. Idealizing the phenomenon, we represent the compression curve of a

*The critical τ_{cr} is understood to be the bulk density at which a zero-th dilatancy effect is assured [1, p. 194; 2, p. 84]. The so-called closest value to it is observed in so-called "compact" moving layers and fluidization at rest [3, 4, p. 489].

†The maximal bulk density τ_{max} delimits loose and compact granular layers; a change in the compactness of the latter occurs not under structural but elastic-plastic deformations of grain pressure [5, p. 19; 6, p. 26].

S. M. Kirov Ural Polytechnic Institute, Sverdlovsk. Translated from Inzhenerno-Fizicheskii Zhurnal, Vol. 52, No. 6, pp. 965-974, June, 1987. Original article submitted March 4, 1986.

0022-0841/87/5206-0695 $12.50

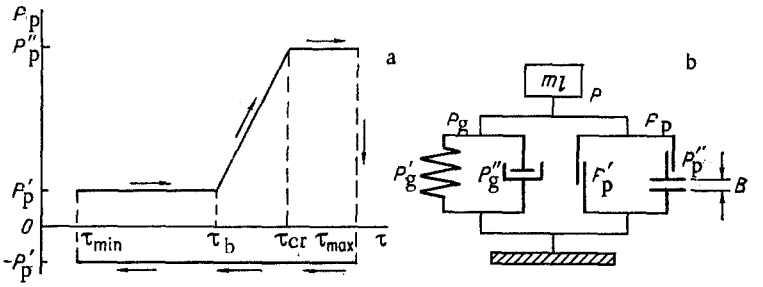

Fig. 1. Idealized compression curve (a) and dynamic model of a loose granular layer (b).

loose layer as consisting of two horizontal sections (Fig. 1a). The presence of the first is due to the existence of numerous different-scale vacancies in the layer for $\tau = \tau_{min} - \tau_b$. The grains on the boundaries with the vacancies are statically unstable and their equilibrium is assured mainly by the action of the internal friction. Upon redislocation in the vacancies, the particles do not disturb their neighbors and do not spoil the further addition of friable medium. In conformity with the Coulomb law the dry friction forces in such a layer comprise an order of several fractions of the normal pressure:

$$P_p = P_p' = \alpha_1 \rho_l g H_l \operatorname{sign}(\dot{X}), \tag{1}$$

where $\alpha_1 \leqslant 0.5$ is the reduced coefficient of internal dry friction [8].

The smallness of the scale of the friction force P_p', the first "yield point" of a loose medium, as compared with the static stresses in indeed the reason for the known low stability of loose layers. Vacancies are rare on the second horizontal section ($\tau_{cr} - \tau_{max}$) and the overwhelming majority of particles is in a statistically stable state. Extrusion of the excess grains is here coplicated by displacement of all their surrounding neighbors and by spoilage of the further addition of friable medium. The "yield point" of such a layer under compression will exceed (and substantially in a number of cases) the static stress. However, in the tension phase of the layer the magnitude of the limit forces of the interparticle interaction again drops to the minimal value (1). This latter is due to the known absence of the ordering phenomenon for a friable medium (without a load) during its vibration impact treatment [5, p. 23; 6, p. 47]. Therefore

$$P_p \begin{cases} P_p'' = \alpha_2 \rho_c g H_l & \text{for} \quad X > 0; \ \dot{X} > 0, \\ P_p' = \alpha_1 \rho_c g H_l & \text{for} \quad \begin{cases} X \leqslant 0; \ \dot{X} < 0, \\ X < 0; \ \dot{X} > 0. \end{cases} \end{cases} \tag{2}$$

Here $\alpha_2 > 1$ is the coefficient of resistance of a friable medium to plastic compression for $\tau > \tau_{cr}$. According to our data, α_2 is practically independent of the kind of material and the particle diameter and is $\alpha_2 \sim 10^3 \alpha_1$ (see Table 1).

Rearrangement from an unstable to a stable structure is realized in the intermediate zone ($\tau_b - \tau_{cr}$) Because of the diminution of vacancies and the compression of the layer, its resistance to compression grows from the level P_p' to P_p''. Because of the large difference between them the transition can provisionally be represented by a straight line. For this zone

$$P_p = \begin{cases} \alpha_{12} \rho_c g H_l & \text{for} \quad X > 0; \ \dot{X} > 0, \\ \alpha_1 \rho_c g H_l & \text{for} \quad \begin{cases} X \leqslant 0; \ \dot{X} < 0, \\ X < 0; \ \dot{X} > 0, \end{cases} \end{cases} \tag{3}$$

where $\alpha_{12} \simeq \alpha_1 + \alpha_2 (\tau - \tau_b)/(\tau_{cr} - \tau_b)$.

Here τ_b is understood to be the bulk density at which the transition from an unstable to an intermediate structure is realized. Taking into account that the range of layer fluctuations (10^0-10^2 Hz) lies significantly below the frequencies of natural elastic vibrations in the layer grains excited during their elastic deformations. the nature of skeleton stress formation in a first approximation can be assaumed quasistationary.

The complete dynamic resistance of a loose granular medium includes viscoelastic in addition to sleketon stress in the continuous (gaseous) phase, whose action under specific condi-

TABLE 1. Properties of Disperse Materials

Material	ρ_b, kg/m³	d_p, μm	ε_0	ε_1	ε_2	ε_3	ε_4	ε_b^*	$\varepsilon_{b\,calc}^*$	ε_{cr}	b_{cr}	α_1	α_2
Cinders Ashes Vorkutinsk TES	2820	0—10	0,720	0,506	—	—	0,543	0,620	0,586	0,560	0,363	0,126	112
Synthetic corundum	1950	0—40	0,630	0,506	0,507	0,576	0,477	0,560	0,543	0,516	0,279	0,162	106
Synthetic corundum	3900	0—40	0,620	0,528	0,514	0,577	0,537	0,613	0,580	0,550	0,266	0,124	98
Synthetic corundum	3900	40—50	0,620	0,515	0,534	0,518	0,433	0,600	0,580	0,550	0,211	0,163	102
Synthetic corundum	3900	100—125	0,588	0,494	0,510	0,490	0,474	0,560	0,558	0,525	0,134	0,126	91
Synthetic corundum	3900	125—160	0,561	0,471	0,506	0,490	0,490	0,550	0,540	0,505	0,114	0,179	106

*Determined for V_0 = 0.77 m/sec.

tions [8] is subjected to the additivity rule: $P = P_g + P_p$ (Fig. 1b). Depending on the initial conditions (τ_0, V_0), different versions of the interaction between a loose fill and an obstacle are possible here, some of which are considered below.

1. A possible elastic deformation of the layer X_m (in the initial velocity level V_0) does not exceed the available compression deformation of the fill in the unstable domain B ($X_m < B$), where

$$B = H_0(1 - \tau_0/\tau_b) = H_0 b. \tag{4}$$

This case is considered in [8], where, in particular, a lower limit condition (V'_{cr}, in the dumping velocities) is formulated for the origin of free elastic vibrations in the loose layer. An upper limit velocity V''_{cr} assuring conservation of the elastic vibrations modes also exists. It is found if we substitute $X_m = B$ in the solution of the equation of motion

$$V''_{cr} = \omega_l B \sqrt{1 + 2\Delta_\tau/B} - \alpha_1 g \tau_v/2. \tag{5}$$

Estimating the limit value for the case H_ℓ = 0.1 m (ash) and taking into account the empirical data presented in the table, we obtain V''_{cr} = 3.7 m/sec.

2. The possible elastic deformation of the layer exceeds the available value: $X_m < B$. Here at the time t_b determined from the condition $X(t) = B = X_b$, the elastic deformation of the layer is replaced by plastic crumpling of the skeleton of the obstacle, the repacking of the particles, and the compression of the layer.

The duration of the crumpling is determined by the time to quench the rate of layer compression to zero (by dissipation of the kinetic energy of the fill $\sim \dot{X}_b^2$ remaining to the time of impact t_b). The maximal compression of the layer is achieved at the end of the plastic impact t_{pl} ($t_{pl} = t_b + \Delta t_{pl}$) and equals the sum of the elastic and plastic deformation

$$\Delta_l = X(t_{pl}) = B + \Delta X_{pl};\ \dot{X}(t_{pl}) = 0. \tag{6}$$

Taking account of the representations [8], the dynamics of the loose layer for $X_m > B$ is described by the known relationship

$$\ddot{X} + \omega_0^2 \tau_v \dot{X} + \omega_0^2 X = -\alpha g, \tag{7}$$

where in the impact phase ($X > 0$, $\dot{X} > 0$)

$$X(0) = 0;\ \dot{X}(0) = V_0, \tag{8}$$

$$\alpha = \begin{cases} \alpha_1 & \text{for } X(t) < B, \\ \alpha_{12} & \text{for } B < X(t) < B_{cr}, \\ \alpha_2 & \text{for } X(t) > B_{cr}, \end{cases} \tag{9}$$

and in the post-impact phase $\begin{Bmatrix} X \gtrless 0;\ \dot{X} < 0 \\ X < 0;\ \dot{X} > 0 \end{Bmatrix}$

$$\alpha = -\alpha_1. \tag{10}$$

Because of the abrupt post-impact diminution in layer stiffness, elastic forces stored for a deformation Δ_c are released, which assures further development of the vibrations (Fig. 2):

$$X = \pm \Delta_T + \Delta_l \Phi \exp(-\delta f_0 t_1) \sin(\omega_l t_1 + \varphi), \quad \dot{X} \gtrless 0,$$
$$P = P_l \Phi \exp(-\delta f_0 t_1) \sin(\omega_l t_1 + \varphi), \tag{11}$$

where

$$\Delta_T = \frac{\alpha g}{\omega_0^2}; \quad P_l = \frac{\pi}{2} P_{pl}; \quad P_{pl} = \frac{\pi}{2} \frac{P_a \Delta_l}{\varepsilon_l H_l}; \quad \omega_l = \beta \omega_0;$$
$$\omega_0 = \frac{\pi}{2} \frac{a}{H_l}; \quad a = \sqrt{P_a/(\rho_l \varepsilon_l)}; \quad t_1 = t - t_{pl}$$
$$\beta = \sqrt{1 - \frac{\omega_0^2 \tau_v^2}{4}}; \quad \delta = \delta_0/\beta; \quad \delta_0 = \pi \omega_0 \tau_v;$$
$$\Phi = \frac{1}{\beta}\left(1 \pm \frac{\Delta_T}{\Delta_l}\right), \quad \dot{X} \lessgtr 0; \quad \varphi = \operatorname{arctg}\left(\beta \frac{2\pi}{\delta_0}\right).$$

If under repeated compression of the fill in the next fluctuation $X_m < B$, the layer, in conformity with (11), performs motion of a series of damped vibrations of the first kind (Fig. 2a). However, another mode is also possible, under which the impact interaction will be followed also in subsequent compressions of the layer (Fig. 2b). The boundary between the single and multiple collisions modes is determined by competition between the impact and viscoplastic deformations in one period of the vibrations

$$\Delta X_{pl} = \Delta X_{vp}, \tag{12}$$

where $\Delta X_{pl} \approx X_b^2/(2\alpha g)$, $\Delta X_{vp} \approx \Delta_l \Phi(1 - \exp(-\delta))$; ΔX_{vp} is the magnitude of the damped vibrations of the layer during one period of its motion (see Fig. 2a).

The density of the fill achieveable under the layer compression Δ_l is not generally limited, and for an appropriate drop in the velocity V_0 an arbitrary, including even ultimately loose ($\tau = \tau_{min}$) layer can be compressed, in particular, to the critical density τ_{cr}. Taking into account that the resistance to compression in the section $\tau_{min} - \tau_b$ is considerably less than in the section $\tau_b - \tau_{cr}$, we estimate this velocity as

$$V_{cr}''' \approx \sqrt{2\alpha_2 g (B_{cr} - B)}. \tag{13}$$

Or for a given initial velocity

$$H_{cr}''' \approx V_0^2/(2\alpha_2 g (b_{cr} - b)), \tag{14}$$

where B_{cr} is determined by (4) under the substitution $\tau_b - \tau_{cr}$. Substituting the empirical data for layers of height $H_l \approx 0.1$ m, we obtain $V_{cr}''' \approx 6.5$ m/sec while $H_{cr}''' \approx 2.35 \cdot 10^{-3}$ m for the collision velocity $V_0 = 1$/sec.

3. In the preceding cases the density of the fill was less than the critical value τ_{cr} in the initial state, which assured the development of a substantial elastic force maintaining further layer vibrations within the limits of the compression deformation $\Delta_l \sim B$. The initial state of granular materials (for instance, not having dustlike fractions or caking in their composition) is often characterized by stable loose packing with $\tau_0 > \tau_{cr}$. The parameter B is here negative by definition, and nevertheless, according to the model under consideration the fill can perform free elastic vibrations even under these conditions despite the absence of elasticity in its skeleton. It is sufficient to set B = 0 in the solution (11) to describe these vibrations. The computation results are presented in Fig. 2c. As is shown, the mode of these primarily impact vibrations is characterized by prolonged initial and even shorter subsequent force pulses separated by an unchanged step.

One of the most essential characteristics of any free vibrations, including of a loose granular layer also, is the conditional frequency ω_c. An analytic expression to compute ω_c in the cases considered above can be obtained easily after compiling a structural formula for the period T_c of the vibrations (Fig. 2). The period of post-impact vibrations is $T_c \equiv T_l$ for elastic-impact vibrations in the single collision mode; the period is not constant under multiple collisions but is close to the period of the first vibration $T_c \approx t_b + \Delta t_{pl} + (3/4)T_l$. In the third primarily impact mode $T_c = \Delta t_{pl} + (3/4)T_l$. Neglecting the time of

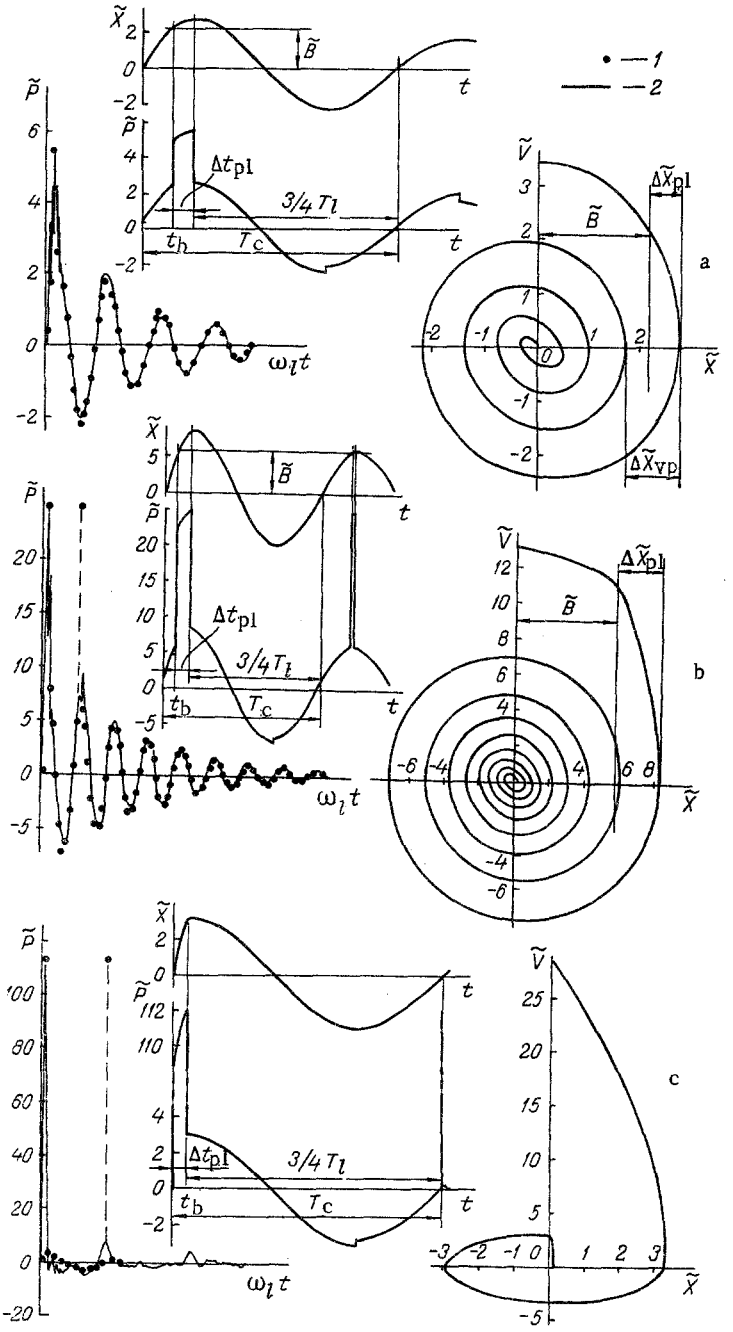

Fig. 2. Phase diagrams of model motion after the drop and the vibrations and pressure fluctuations developed therein; comparison of computed (1) and experimental (2) curves of the total pressure variation in a layer in time: a) fluctuations in the transition zone ($\tau_b \lesssim \tau_0 < \tau_{cr}$) in the single collision mode (corundum, d = 20 μm; H_l = 0.096 m; V_0 = 0.2 m/sec; ε_l = 0.616, ε_b = 0.613, α_1 = 0.124; α_{12} = 5.5); b) in the multiple collision mode (corundum, d = 20 μm; V_0 = 0.767 m/sec; H_l = 0.097 m; ε_l = 0.621; ε_b = 0.613; α_1 = 0.124; α_{12} = 25); c) fluctuations in a stable loose layer for $\tau_0 > \tau_{cr}$ (cinders, d = 10 μm; H_l = 0.051 m; V_0 = 0.767 m/sec; ε_l = 0.517; α_1 = 0.126; α_{12} = 112).

the plastic collision Δt_{pl} as compared with the post-impact part of the process in the last expression, we obtain a simple but quite accurate (with a ~5% margin) characteristics of the limit level of the frequencies in loose layers $\omega_c \approx (3/4)\omega_l$. Performing linear interpolation on the basis of approximate computations, we represent the dependence of the frequency on the density of the fill in the multiple collision mode by the dependence $\omega_c = (1 + (\tau - \tau_{vp})/(\tau_{cr} - \tau_{vp})/3)\omega_l$. Here τ_{vp} is found from the solution of (12). The difference between τ_{vp} and τ_b does not exceed 15-20%, which permits it not to be taken into account. Then the natural vibrations frequency of loose fine-grained layers is determined by the approximate dependence

$$\frac{\omega_c}{\omega_l} = \begin{cases} 1 & \text{for } \tau_0 < \tau_b, \\ 1 + (\tau_0 - \tau_b)/(\tau_{cr} - \tau_b)/3 & \text{for } \tau_b < \tau_0 < \tau_{cr}, \\ \frac{4}{3} & \text{for } \tau_0 > \tau_{cr}. \end{cases} \quad (15)$$

Experimental confirmation of the model was confirmed (Fig. 3a) by a standard method is recording of the response of a characteristic dynamic parameter of the system, the total pressure P (5) and its gaseous P_g (7) and skeleton P_p (6) components to a dosed disturbance under tenfold changes in the particle diameter of the layer in this case. Starting from general considerations, the dissipative losses in loose granular media should be close to the losses in porous vibration-insulated materials. Free vibrations can be excited in such media only under sufficiently good agreement between the duration of the impact pulse and the period of its propagation in the layer. These requirements are satisfied most simply when using the method of a reversed impact action when the vessel 1 with the friable material 2 is dropped along the guide 3 into the support slab 4. The height of the drop h (0.002-0.32 m) governs the collision velocity $V_0 \approx \sqrt{2gh}$ (0.2-0.25 m/sec). The velocity range is analogous to the vibration liquefaction velocities [9]. Readings of the strain gauge resistance pressure sensors 5-7 were recorded by using a mirror-galvanometer oscilloscope H-115. To avoid signal distortion in the sensors the main elements of the apparatus 1, 4 were of lead and their mass exceeded the mass of the primed grains by an order of magnitude. This latter permitted representation of the impact losses in the vessel by plastic fill that excerted no influence on the dynamics. The tests were conducted under normal conditions with materials whose properties are presented in the table.

The initial porosity ε_0 of the fill, corresponding to random loose packing [4, p. 484], was obtained by rapid charging a batch of material into the vessel 1 and light two- or three-time tapping. The H_0/D relationship was usually kept greater than 1 (1-5.5) in the tests, which permitted the excitation mainly of the required longitudinal (vertical) vibrations and

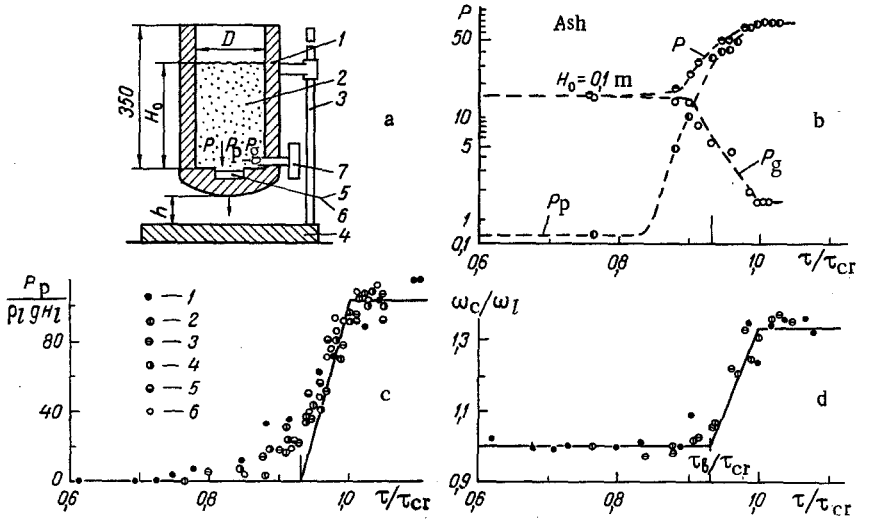

Fig. 3. Diagram of the apparatus (a); experimental dependences of the pressure components (b): (1 — cinders; 2 — ashes; 3 — corundum; d = 20 μm, 4 — 45; 5— 110; 6— 140) and free vibrations frequency (d) (see Fig. 3c for notation) on the bulk density of the layer for V_0 = 0.767 m/sec; solid curves for c and d correspond to a computation according to (3) and (15), P, kPa.

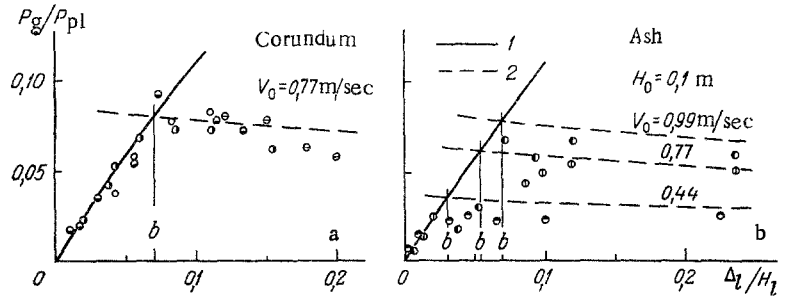

Fig. 4. Dependences on gas pressure in the layer on its deformation for different particle diameters (a) (see Fig. 3c for notation), and collision velocities (b); 1) computation using (120); 2) computation using [8]; a) corundum; b) ashes.

suppression of the transverse. As H_0/D increased from 0.5 to 2 the value of ε_0 diminished somewhat (1-3%) and then stabilized. This range of values is also presented in the table. The porosities ε_b and ε_{cr} were determined by an abrupt change in the gas and particle pressure during compression of the layer (Fig. 3b). The values of ε_0, ε_b, and ε_{cr} were stably repeated from test to test with practically no scatter, which permitted their being considered as structural characteristics of the loose layer. The limiting compression of the materials producible by the recommended methods, impact [10, p. 258; 11] ε_1 and vibrational [6, p. 42; 10, p. 258, 11], ε_2, as well as by pouring water ε_3 and wave ε_4, was quite remote from the maximal τ_{max} [1-6, 10]. The last method afforded the deepest compression when transverse vibrations were excited in the fluid above the granular layer. However, judging by the data [10, p. 259], even when using it the maximal compression is possible only for a substantially longer duration in conducting the process than in the test (hours). Under vibrational compression of the layer the porosity ε_2 approximates the critical value ε_{cr}. The lower level of vibrational impact compression becomes no surprise if the vibrational unhardenability of a friable medium due to the dilatancy effect is recalled. In particular, this means that the production of packing by a dynamic method that is substantially more compact than the critical is possible only upon conserving the smallness condition for the scale of the shear deformation excited here as compared with the characteristic sizes of the granular medium elements. Consequently, the layer density closest to the maximum will be achieved under vibrational compression upon satisfying the condition $A/d_p \ll 1$, which corresponds to the kilohertz frequency band of mechanical or acoustical action ($\geqslant 10^4$ kHz). Information about deeper compression by superposition of an ultrasound field [6, p. 63; 12]* than of low-frequency vibrations [6, 9-11] can be a confirmation.

The test results are confirmed by developed model representations. A typical compression curve for the class of disperse materials under consideration and data on the size of the pressure components indicate the presence of the three loose layer zones discussed above, as well as the real existence of a balance of forces $P = P_g + P_p$ in each of them (Figs. 3b and c). The properties of the granular material (d_p, ρ_p) do not noticeably affect the magnitude of the inter-particle interaction forces P_p, which is substantially a function of the mean bulk density of the friable medium and the disturbing action (V_0). In its turn, the parameters P_g and P depend essentially on the mechanical and dynamical characteristics of the system.

As was assumed, each of the three zones of the compression curve for a loose layer has its inherent characteristic type of layer reaction to impact action that entirely corresponds to the model modes described above. For reactions of the first kind that occur in the loosest layers of low height and for comparatively low values of V_0, the total pressure sensor records practically smooth, flat, weakly damped curves [8] after the time when the vessel meets the support slab. As the particle size, collision velocity, and initial density τ_0 increase in the first half-period of layer interaction with the bottom, a quite-definite "hard" impact pulse appears that grows proportionately to the bulk density of the fill. In subse-

*The frequency band of mechanical action (up to 30 kHz) mentioned in the survey [2] is erroneously exaggerated (by 100-fold) versus the original. Consequently, the data cited in [2, p. 173] are not discussed here.

quent half-periods the impact interaction is either not detected (see Fig. 2a) or traced even further (see Fig. 2b). In the third case, the main part of the energy is dissipated in the first impact after which weakly defined vibrational motions follows (see Fig. 2c). The free vibrations frequencies determined in the tests are in good agreement with the estimates made by means of (15) (Fig. 3d), where the vibrations themselves are observed both in the unstable and stable granular layers whose deformative properties seem to be quite negligible. Certain deviations of the computed pressure values from the experimental (Figs. 2c and d) can be associated with both the constraint of the fast-response of the strain-gauge pressure sensors comprising $\sim 10^3$ Hz according to [13, p. 59] and the possible dependence of the coefficient α_2 on the impact velocity of the type "structural viscosity" [6, p. 40]. However, the latter requires special refinement.

In particular, the detected regularities permit representation of the evolution of the forced vibrations, described in [9], for fine-grained fills as their mean porosity varies between $\varepsilon \leq \varepsilon_{cr}$ and $\varepsilon \simeq \varepsilon_{max}$ as the successive replacement of vibrations modes by starting from primarily an impact mode and ending with an elastic mode accompanying a 30% diminution in the resonance height of the fibration layer in the transition zone. The appearance of "inconceivable" resonance frequencies of 150-250 Hz in vibration-compressed low (<0.1 m) layers of fine-grained materials [6, p. 52] quite remote from the elastic vibrations frequencies of compact granular systems and exceeding the frequency of resonance elastic vibrations being developed in unstable loose structures by 1.5 times can be due to those same (impact) vibrations.

A comparison of experimental data on gas pressure with computations indicates the good convergence of the model representations to experiment (Fig. 4). The excess of the experimental values ε_b over the computed is 0.5-6.0% (see Table).

NOTATION

A, vibrations amplitude; B, b, absolute, relative available deformation of the layer; D, d, apparatus and particle diameters; f, vibrations frequency; g, free-fall acceleration; H, h, height of the layer and the drop; P, pressure; T, period of the vibrations; t, Δt, time and time interval; V, collision velocity; X, instantaneous deformation of the layer; ΔX, finite deformation of the layer; $\dot{X}$, instantaneous deformation rate of the layer; α, reduced friction coefficient; Δ, absolute deformation; ε, porosity; ρ, density; $\tau = 1 - \varepsilon$; bulk density; τ_v, particle velocity relaxation time; $\omega = 2\pi f$; angular frequency. $\tilde{P} = P/\rho_c g H_c$; $\tilde{X} = X\omega_0^2/g$; $\tilde{B} = B\omega_0^2/g$; $\tilde{V} = V\omega_0/g$, dimensionless parameters. Subscripts, cr, critical; m, max are maximal; min, minimal; B, deformation B; p, particle; l, layer or free; g, gas; 0, initial parameters, intrinsic; f, friction; pl, plastic; vp, viscoplastic; c, conditional.

LITERATURE CITED

1. M. A. Gol'dshtik, Transport Processes in a Granular Layer [in Russian], Novosibirsk (1984).
2. A. D. Zimon and E. I. Andrianov, Autohesion of Friable Materials [in Russian], Moscow (1978).
3. P. N. Platonov, Inzh.-Fiz. Zh., 12, No. 6, 807-811 (1967).
4. J. Happel and G. Brenner, Hydrodynamics at Low Reynolds Numbers [Russian translation], Moscow (1976).
5. G. K. Klein, Structural Mechanics of Friable Bodies [in Russian], Moscow (1977).
6. I. G. Shatalova, N. S. Gorbunov, and V. I. Likhtman, Physicochemical Principles of Vibrational Compression of Powder Materials [in Russian], Moscow (1965).
7. Yu. A. Buevich, Inzh.-Fiz. Zh., 40, No. 1, 61-69 (1981).
8. A. F. Ryzhkov and B. A. Putrik, Inzh.-Fiz. Zh., 52, No. 5, 795-802 (1987).
9. E. F. Karpov, A. S. Kolpakov, B. A. Putrik, et al., Physicochemical Gasdynamics [in Russian], Sverdlovsk (1985), pp. 97-106.
10. D. D. Barkan, Vibration Method in Construction [in Russian], Moscow (1959).
11. T. Yoshida and Y. Kousaka, Chem. Eng. Jpn., 5, No. 1, 159-163 (1967).
12. R. D. Morse, Ind. Eng. Chem., 47, No. 6, 1170-1179 (1955).
13. N. F. Krasnov (ed.), Applied Aerodynamics [in Russian], Moscow (1974).